

Structure for an LHC 90mm Nb₃Sn Quadrupole Magnet

A.R. Hafalia, S. Caspi, S.E. Bartlett, D.R. Dietderich, P. Ferracin, S.A. Gourlay, C.R. Hannaford, H. Higley, A.F. Lietzke, B. Lau, N. Liggins, S. Mattafirri, A.D. McInturff, M. Nyman, G.L. Sabbi, R.M. Scanlan, and J. Swanson

Abstract— A full-scale mechanical model of the LHC Nb₃Sn quadrupole magnet structure has been designed, built and tested. The structure will support a 90mm bore, 1m long magnet prototype as part of the US LHC Accelerator Research Program (LARP). The structure utilizes Bladder and Key Technology to control and transfer pre-stress from an outer aluminum shell to an inner coil. Axial aluminum rods take care of pre-stress at the ends - ensuring that the coil is fully constrained along all three axes. The outer aluminum shell and an inner “dummy coil” (aluminum tube) were extensively instrumented with strain gauges. The gauges were used to monitor and map the effectiveness of the stress relation between the loading structure and a “dummy” coil through varying mechanical load conditions – from bladder and key pre-stress at room temperature through cool-down. Test results of the stress distribution in the structure and the in dummy coil is reported and compared with expected results calculated with the structural analysis program ANSYS.

Index Terms—Bladders, Keys, Nb₃Sn, Quadrupole

I. INTRODUCTION

THE Superconducting Magnet Group at Lawrence Berkeley National Laboratory is applying a new magnet loading structure to a quadrupole magnet. The loading structure provides efficient containment of large Lorentz forces generated by a high field, Nb₃Sn superconducting accelerator magnet. The aluminum shell/iron yoke load structure design and Bladder & Key Technology [1] have successfully been proven on record-breaking dipole magnets - i.e., RD-3B “Racetrack Dipole” Magnet (13.5T) [2], and, more recently, the HD-1 “Block Dipole” (16T) [3]. The Nb₃Sn Interaction Region (IR) Quadrupole upgrade proposal for the LARP program has enabled the group to branch out and explore the application of this structure on a cosine-2Q magnet design.

The aluminum shell/iron yoke design is a more efficient way of preloading high field magnet coils (>10T) than the keyed-collars commonly used in production accelerator magnets (<10T). In the keyed-collar system, the hydraulic

press must overshoot the final prestress for the coil to install the locking keys. A considerable amount of this initial loading is lost when the hydraulic pressure is released to allow the locking keys to seat in the collars. Also, these types of collar structures experience prestress loss during cool-down. In the aluminum shell/iron yoke system, the room temperature preload required to assemble the shell, yoke, bladder & key structure around the magnet coils is only 30%-50% of the final preload. This final preload is attained by using water-pressurized internal bladders placed between the coilpack and yokes - stretching the aluminum shell while compressing the coils. Interference load-keys are placed between the yokes and the coilpack [2]. Deflating the bladders allows the stretched aluminum shell and yokes to seat against the load keys, imparting the required room-temperature preload to lock the assembly together. At this point, the bladders are removed for possible re-use. Final preload is attained after the magnet assembly has been cooled down to cryogenic temperatures as the aluminum cylindrical shell contracts more than the iron and stainless steel inside it – doubling the room temperature preload.

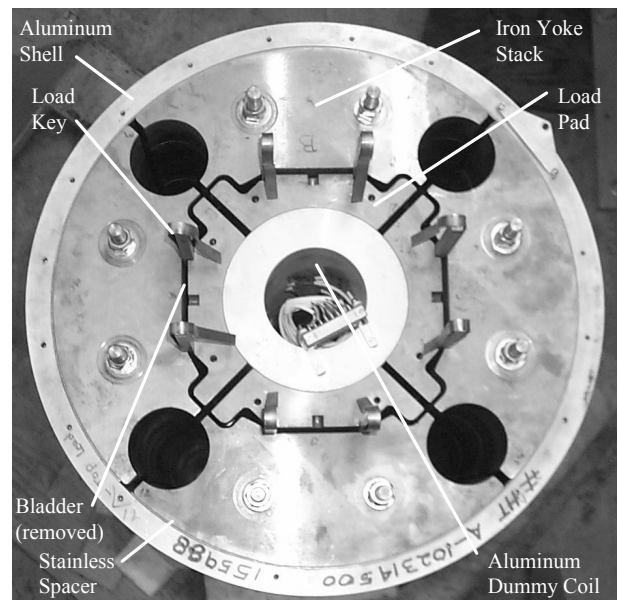


Fig. 1. Photo of the IR Quad structure showing instrumented “dummy coil”.

Manuscript received October 5, 2004. This was supported by the Director, Office of Energy Research, Office of High Energy and Nuclear Physics, High Energy Physics Division, U. S. Department of Energy, under Contract No. DE-AC03--76SF00098.

All authors are with the Lawrence Berkeley National Lab, Berkeley, CA 94720 USA (telephone: 510 486 5712, e-mail: rrhafalia@lbl.gov).

II. BASIC DESIGN

The main components of the structure are the four iron yoke-stack quadrants, symmetrically spaced inside a 6061-T6 aluminum cylindrical shell (Fig.1).

Each yoke stack is made up of ten 50.8 mm-thick steel laminations, precision machined and assembled together with tie-rods. Each stack weighs 211 kg (465 lbs). Yoke profiles are cut such that clearance cavities are made for the coil pack and four structural aluminum, axial loading tubes. For this first phase of the structural testing, axial loading was not performed.

A 1.6mm-thick rolled-steel sheet was sandwiched between the shell inner surface and the yoke outer surfaces – acting as a skin. In a future design iteration, this skin will be replaced by a welded stainless steel pressure vessel that will serve as an integrated cryostat.

The coil pack is composed of four stainless steel load pads bolted around the coils. This makes up a unitized sub-assembly prior to insertion into the shell/yoke loading structure.

For this first phase of structural testing, a strain gage-instrumented “dummy” coil, made from a machined aluminum tube, was used to simulate the quadrupole coil assembly.

III. STRAIN GAGE INSTRUMENTATION AND TRACES

Strain gages were placed on the shell external surface and the dummy coil bore surface at the positions corresponding to the pole and mid-plane locations in a quadrupole magnet.

A. Aluminum Shell Instrumentation

Integrated full-bridge strain gages were compared with half-bridge strain gage pairs. Each half-bridge strain gage was temperature compensated by another half-bridge gage on an aluminum, floating pad. The shell strains were measured in ϵ_θ -azimuthal strain, ϵ_z -axial strain and $(\epsilon_\theta - \epsilon_z)$. Gages were arrayed into four azimuthal stations around half of the shell, two over pole and two over mid-plane locations – making up the “Type A” trace assembly (Figs. 2&3). Each four “fingers” of the Type A trace assembly held one full-bridge gage, one half-bridge gage (oriented to read azimuthal strain) and another half-bridge gage (oriented to read axial strain). The “Type B” trace assembly had half-bridge strain gages at its four stations around the other half of the shell – all reading azimuthal strains.

A precision photo-etched copper/kapton trace was designed and made to bring the signals from the strain gage arrays to a convenient and common location on the shell.

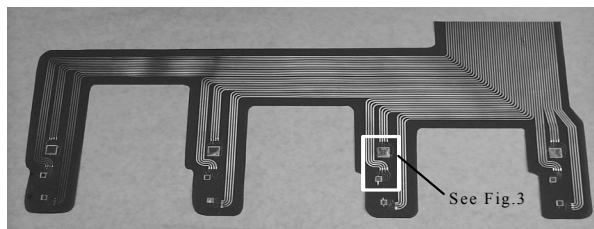


Fig. 2. Copper/Kapton photo-etched trace for aluminum shell.

The individual gages were pre-soldered onto the traces via 32 Ga. insulated copper wire jumpers, laying flat on the workbench. The trace was, then, bonded to the curved surface of the shell. The trace unitizes the strain gage array so that installation and instrumentation cable hook-ups are facilitated. To install 16 strain gages individually would have been time consuming. Because the special strain gage bonding agent required oven-curing within thirty minutes after application, pre-mounting the gages on the trace facilitated the installation of the whole array.

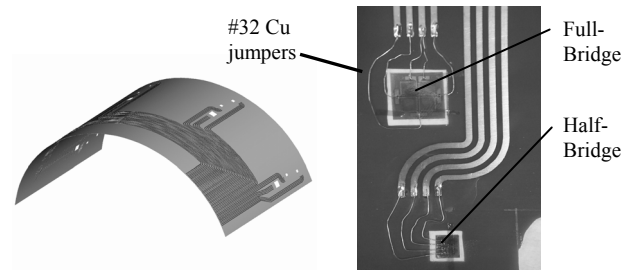


Fig. 3. CAD model of the Type A trace (left) and close up of gage installation (right). The temperature compensating strain gages were soldered onto the half-bridge after the trace was bonded and cured on the shell surface.

The trace routes brought the terminus of each gage to a localized and common region of the shell where jumpercables connected the trace to a centralized set of Hypertronics connectors (Fig. 4).

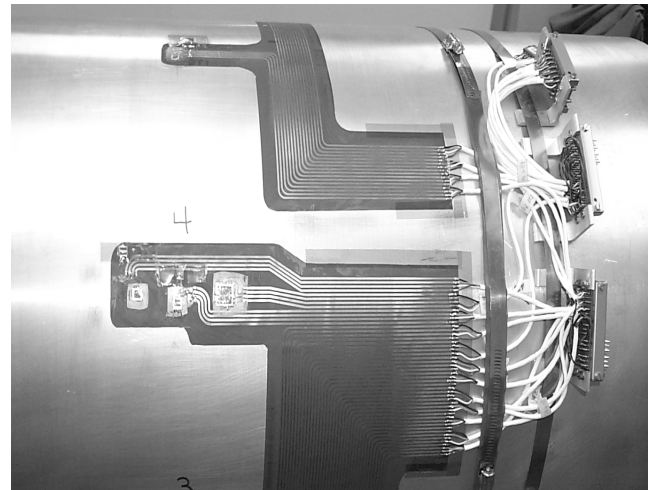


Fig. 4. Shell trace assemblies installed and wired to connectors. The Type A trace assembly is shown on the bottom half of the shell and the Type B trace assembly on the top half.

B. Dummy Coil Instrumentation

A 6061-T6 aluminum 2-piece tube machined to an outer diameter of 160.71mm and an inner diameter of 90mm and 1016mm length, was used to simulate an assembled quadrupole coil. Full-bridge strain gages were placed within the bore, using a similar trace design as the shell (Fig. 5). A special compression fixture (Fig. 6) was designed to press the trace and gages against the bore surface of the dummy coil to properly place them during the oven-curing process.

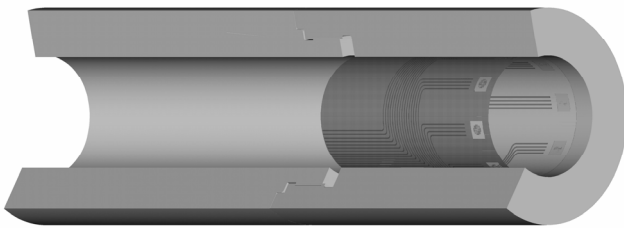


Fig. 5. Cut-away CAD model of the dummy coil's bore strain gages.

Flexible steel shim stock was used as leaf-springs to provide the outward pressure on the rubber contact pads. The ends of the leaf-springs were attached to aluminum end plates. The end plates were drawn together by a threaded rod to deflect the springs outward, against the bore surface.

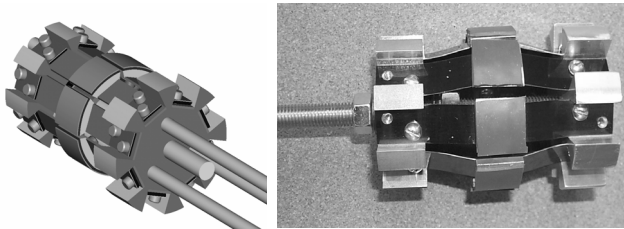


Fig. 6. CAD model of Bore strain gage compression fixture (left); photo of actuated, actual fixture (right).

The fixture and strain gage trace were installed in the aluminum dummy coil and seem to have performed well during curing process. After curing, it was observed that three of the eight bore gages were only partially bonded against the bore. The gages were hooked up to monitoring equipment and an LN₂ “dunk” test was performed on the dummy coil. All 8 gages were active, but the same three indicated ineffectiveness.

IV. DUMMY COIL-PACK PRE-ASSEMBLY

After the dummy coil was instrumented and assembled, the load pads were assembled around it and bolted together to make up the “coil pack” (Fig. 7). Care was taken to plumb and level the load pads during the torque sequence so that the assembled coil pack was close to the target dimensions. The objective in assembling the coil-pack was to attain a square cross-section so the room temperature pre-loading in the loading structure will impart a symmetrical and uniform load on the dummy coil.

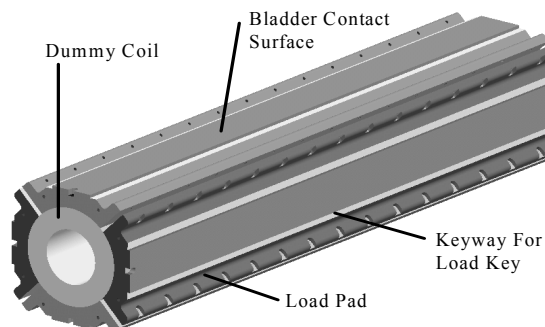


Fig. 7. CAD Image of Assembled “Coil Pack”.

V. ROOM-TEMPERATURE PRELOAD PROCESS USING BLADDERS AND KEYS

The pressurized bladders act as internal presses, stretching the outer aluminum shell by pushing against the yokes and compressing the coils by reacting against the coil pack. This creates clearance for the insertion of the load keys. The keys were shimmed to a prescribed interference thickness that imparted the target room temperature preload on the “coil pack” after the bladders were de-pressurized. The four 69.8 mm x 1016.0 mm bladders were individually pressurized to facilitate interference load key and shim installations per quadrant. The goal was to end up with the same key thickness at all 2x4 key locations. To reduce bladder pressure to stay within the safe limits of the pump, the coil pack was preloaded using three intermediate key sizes. Each intermediate key size was introduced in sequence. After a key-pair in one quadrant was inserted, the opposite quadrant was then pressurized and preloaded, and so on. During this process, all the strain gage arrays on the shell and dummy coil were continuously monitored.

With the introduction of the final key size and the outer shell attaining its prescribed design strain values (determined by ANSYS), the bladders were deflated and pulled out. Fig. 8 plots strain from representative strain gage data measured on the shell and the dummy coil during the loading of the first intermediate key size.

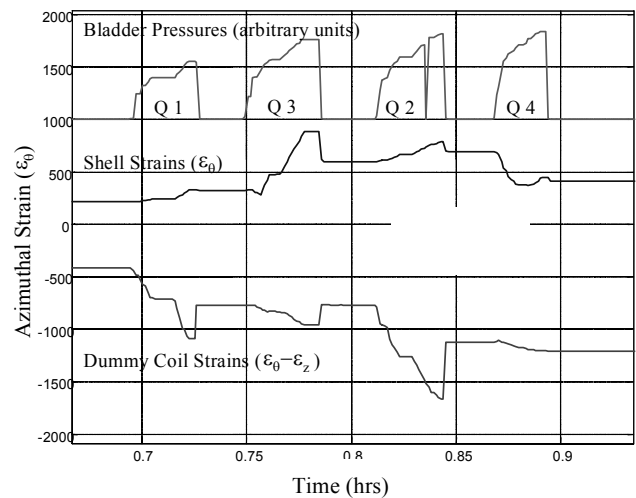


Fig. 8. Measured azimuthal strain sequence in the shell and dummy coil while loading the first intermediate key size. Note the correlation of the shell strains (tension-positive), dummy-coil strains (compression-negative) and the bladder pressurization in each quadrant (Q1-Q4).

VI. COLD TEST AND RESULTS

The final structural assembly was mounted on our 813 mm diameter magnet test cryostat and cooled to 80K with LN₂. Strain gauge measurements have been compared with the results of a 3D finite element ANSYS model. The model, described in detail in [4] (Fig. 9), computed the strain in the shell and the dummy coil after assembly and during cool-down. Contact elements were inserted between all the

surfaces. “Frictionless” and “with friction” conditions were analyzed.

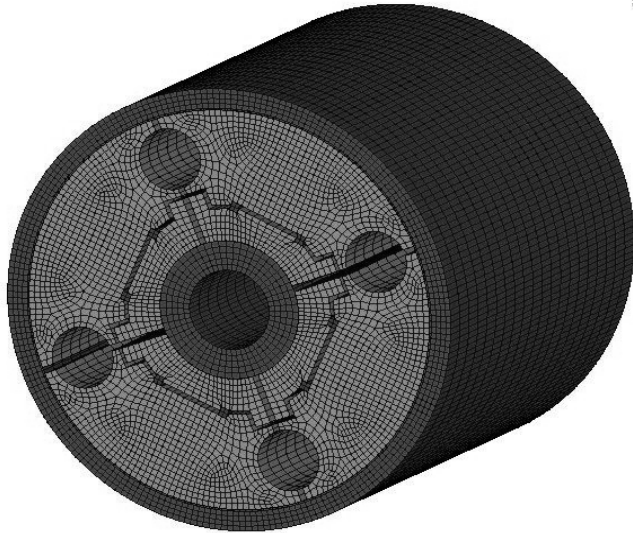


Fig. 9. 3D finite element model of the mechanical structure

In Fig. 10 the azimuthal strain in the shell, as a function of key interference, is plotted: the measurements taken from the shell half-bridge strain gauges show that, at room temperature, 0.43 mm interference key produces a shell strain variation of 1100 microstrain (77 MPa). During cool-down, an increase of 1000 microstrain (80 MPa) is recorded. The computations

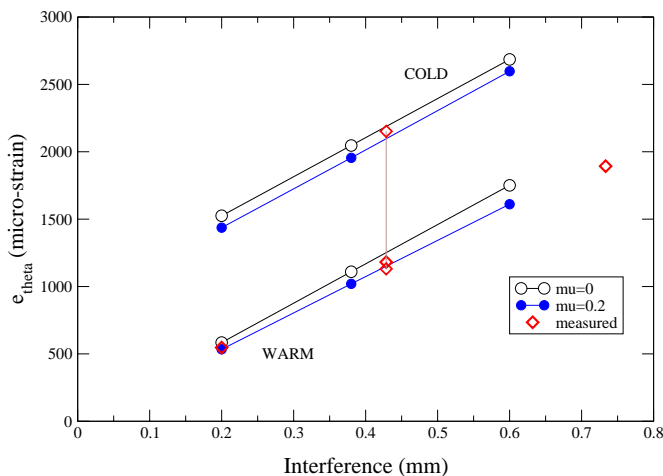


Fig. 10. Averaged azimuthal strain in the shell versus key interference at the third and final cycle. Numerical computations (frictionless and with friction) and experimental data are shown. The analysis shows no significant impact of friction.

Along the axial direction, the measurements taken by half-bridge gauges showed unreasonably high values of tension in the shell. These values were inconsistent with both numerical results and with measurements taken by full-bridge gauges in the same locations. Investigations are currently under way.

The load keys (between load pads and yokes) compressed dummy coil along the azimuthal direction. At the same time, the compression produced a Poisson-effect elongation along

the axial, Z-axis. This behavior is depicted in Fig. 11, where the difference between azimuthal (compression-negative) and axial (tension-positive) dummy coil strain is plotted, for both model and experimental data (full-bridge gauges). During cool-down, friction between pad and dummy coil prevented the latter from contracting freely, thus producing an increase of dummy coil axial tension. This effect explained the large strain variation measured during cool-down by the gauges

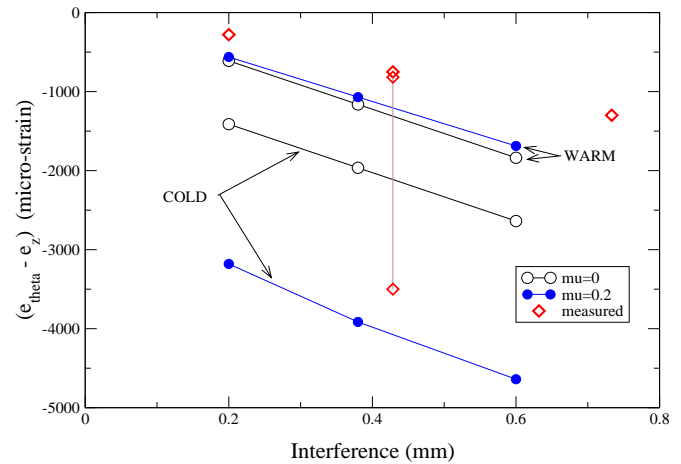


Fig. 11. Difference between azimuthal and axial strain in the dummy coil versus key interference: numerical computations (frictionless and with friction) and experimental data.

VII. CONCLUSIONS

The loading structure’s aluminum components’ stress interactions were studied. Both outer shell and dummy coil were instrumented with strain gauges mounted on copper/kapton traces to facilitate the installation. The structure was loaded at room temperature and cold tested cold to 80 K. The experimental data was compared with the 3D ANSYS computations. The numerical analysis’ results were in agreement with the strain gage measurements, which indicated an increase of shell azimuthal stress during cool-down of about 80 MPa. A significant friction contribution on dummy coil axial tension was also realized.

REFERENCES

- [1] S. Caspi et al., “The use of Pressurized Bladders for Stress Control of Superconducting Magnets”, *IEEE Trans. Appl. Supercond.*, Vol. 11, no. 1, March 2001, pp. 2272-2275.
- [2] R.R. Hafalia et al., “A new support structure for high field magnet”, *IEEE Trans. Appl. Superconduct.*, Vol. 12, no. 1, March 2002, pp. 47-50.
- [3] R.R. Hafalia, et al, “HD-1: Design and Fabrication of a 16 Tesla Nb₃Sn Dipole Magnet”, *IEEE Trans. Appl. Supercond.*, vol. 14, no. 2, October 2003, pp. 283-286.
- [4] S. Caspi, et al., “Mechanical design of a second generation LHC IR quadrupole”, *IEEE Trans. Appl. Supercond.*, Vol. 14, no. 2, June 2004, pp. 235-238.